The maize brown *midrib6* (*bm6*) mutation encodes a functional *GTP Cyclohydrolase1*

April Leonard[1] Orcid, Shuping Jiao[1] Orcid, Lynn Heetland[1] Orcid, Jennifer Jaqueth[1] Orcid, Tiffany Hudson[1] Orcid, Kevin D. Simcox[1,2] Orcid, Robert B. Meeley[1,2] Orcid, Dilbag S. Multani[1,2] Orcid

[1] Corteva Agriscience, 7300 NW 62nd Avenue, P. O. Box 1004, Johnston, Iowa 50131 USA

[2] (KDS) West Des Moines, Iowa USA; (RBM) Des Moines, Iowa USA; and (DSM) Napigen Inc., 200 Powder Mill Road, Delaware Innovation Space – E500, Wilmington, Delaware 19803 USA

*Corresponding author: E-mail: dilbagmultani8@gmail.com

Keywords: *brown midrib6 (bm6), Map-based cloning, GTP Cyclohydrolase1, Silage*

Abstract

Brown midrib mutations in maize (*Zea mays* L.) and sorghum (*Sorghum bicolor* L.) alter lignin composition and enhance cell wall digestibility. These mutations are prime candidates for silage breeding. Six *brown midrib* mutants are currently known, *brown midrib1* (*bm1*) to *brown midrib6* (*bm6*). The *bm1* and *bm3* mutations are being used commercially for silage. The underlying genes responsible for five of the six bm mutations in maize (*bm1*, *bm2*, *bm3*, *bm4*, and *bm5*) are known. Chen and co-workers (2012) characterized the *bm6* mutation, demonstrating that *bm6* increases cell wall digestibility and physically mapped *bm6* within a 180 kilobase region on chromosome 2. The present investigation utilized map-based cloning to identify the candidate gene responsible for the *bm6* phenotype as GTP Cyclohydrolase1 (GCH1) and validated the candidate gene through reverse genetics. Orthologs of *bm6* include at least one paralogous gene in maize on chromosome 10 and various homologs in other grasses and dicots. The discovery that GCH1 is responsible for the maize *bm6* phenotype suggests that GCH1 plays a role in the tetrahydrofolate biosynthetic process.

Abbreviations

4CL1 - 4-coumarate coenzyme A ligase1
bm - Brown midrib mutants
BMR - Brown midrib mutants in sorghum
CAD - Cinnamyl alcohol dehydrogenase
COMT - Caffeic acid O-methyltransferase
FPGS - Folylpolyglutamate synthase
gDNA - Genomic DNA
GSP - Gene-specific primer
GCH1 - GTP Cyclohydrolase1
KASP - Kompetitive allele-specific PCR
MTHFR - Methylenetetrahydrofolate reductase
Mu – Mutator
Mu - TIR - Mutator-terminal inverted repeat
NSS - Non-stiff stock elite inbred line
PCR - Polymerase Chain Reaction
PPTM - Part per ten million
RT-PCR - Reverse Transcriptase-polymerase chain reaction
SAM - S-adenosyl-L-methionine
SNP - Single Nucleotide Polymorphism
SSR - Single Sequence Repeat
TUSC - Trait Utility System for Corn.

Introduction

In North America, maize has been cultivated mainly for grain production for thousands of years. Maize has also been used for forage as its quality is relatively consistent, and its yield and energy contents are high (Lauer, 1995). The USA is the largest maize forage producer globally (Lauer *et al.*, 2001). Cell wall digestibility is the key factor in determining forage quality (Andrieu *et al.*, 1993; Barrière *et al.*, 2003, 2004a). Despite forage yield improvements of 0.13 to 0.16 t/ha per year since 1930, there has been no improvement in cell wall digestibility (Lauer *et al.*, 2001). In Europe, maize is widely grown as a forage crop with ~4.6 mha surface area coverage (Barrière *et al.*, 2004a). Breeding efforts in Europe have substantially improved whole plant yield over the last decade, with ~0.1 t/ha increase per year overall. However, cell wall digestibility substantially decreased over this time, which has resulted in a reduced feeding value of elite maize hybrids (Barrière *et al.*, 2005). Cell wall digestibility correlates highly with biomass quality for forage (Barrière *et al.*, 2003, 2004b) and cellulosic ethanol production (Lorenz *et al.*, 2009). Lignin limits the access of cellulolytic enzymes to the cell wall (Moore and Jung, 2001), and a negative correlation exists with lignin content and either in vitro or in vivo cell wall digestibility (Riboulet *et al.*, 2008). Lignin, cross-

Table 1 - A list of Kompetitive allele-specific PCR primers (KASP markers) used to narrow down the chromosomal region associated with the *bm6* locus in a fine-mapping population.

KASP Primer	Sequence (5' - 3')
PZE-102006385_A1	GAAGGTGACCAAGTTCATGCTGATTTTGGTTTGCAGCCTCCGGA
PZE-102006385_A2	GAAGGTCGGAGTCAACGGATTTTGGTTTGCAGCCTCCGGG
PZE-102006385_C1	GCAAGCAAAATACTCCTATGTGCAACAAA
PZB01233.2_A1	GAAGGTGACCAAGTTCATGCTTCCATAGTTCCATGACGAGAATTCAT
PZB01233.2_A2	GAAGGTCGGAGTCAACGGATTCCATAGTTCCATGACGAGAATTCAG
PZB01233.2_C1	GCGCGACGCAAGCTGCCACT
PUT-163a-60346233-2546_A1	GAAGGTGACCAAGTTCATGCTAAAAAAATAACAGCTTATAAGATGCGCCT
PUT-163a-60346233-2546_A2	GAAGGTCGGAGTCAACGGATTAAAAATAACAGCTTATAAGATGCGCCC
PUT-163a-60346233-2546_C1	ACTGAGGGCACTAGACGAGGCA
PZE-102007336_A1	GAAGGTGACCAAGTTCATGCTTTCTTCTCTTCCGTCTATCTAATCA
PZE-102007336_A2	GAAGGTCGGAGTCAACGGATTTCTTCTCTTCCGTCTATCTAATCG
PZE-102007336_C1	GCAAATCAGCAAATCATCAGCTGGCA
bm6_3708522_A1	GAAGGTGACCAAGTTCATGCTGAACACAAGTAATTTGATTAATACCTATACG
bm6_3708522_A2	GAAGGTCGGAGTCAACGGATTGAACACAAGTAATTTGATTAATACCTATACT
bm6_3708522_C1	GGGCGCAAACATTTTGTGTATCTCTTAT

linked with arabinoxylans through ferulate bridges, is a heteropolymer that strengthens stalks and is essential for water transport in vascular tissue and resistance to pathogens in higher land plants (Baucher *et al.*, 1998; Boerjan *et al.*, 2003; Weng and Chapple, 2010). In maize, lignin polymers are composed of the three different hydroxycinnamoyl alcohol subunits (monolignols), p-coumaryl, coniferyl, and sinapyl alcohol (Barrière *et al.*, 2007). Lignin structure affects cell wall digestibility, for example, the ratio of syringyl (S) to guaiacyl (G) units (Grabber *et al.*, 2004; Barrière, 2017). Both lignin content and ferulate-lignin cross-linking have more impact on cell wall digestibility than lignin composition (Grabber *et al.*, 2009).

Brown midrib (bm) mutants contain reddish-brown pigmentation in their leaf midribs (Sattler *et al.*, 2010). First reported over 90 years ago (Jorgenson, 1931), the association of the reddish-brown bm leaf phenotype is well established with reduced lignin concentration in maize (Grand *et al.*, 1985; Cherney *et al.*, 1991; Sattler *et al.*, 2010). Maize contains six known brown midrib loci. Based on map locations and non-allelic relationships in crosses among each other, these recessive mutations are *bm1*, *bm2*, *bm3*, *bm4*, *bm5*, and *bm6*. The *bm1* to *bm4* mutants have reduced lignin content, altered composition, and increased cell wall digestibility (Barrière *et al.*, 2004b). *bm1* and *bm3* encode the lignin biosynthetic enzymes cinnamyl alcohol dehydrogenase (CAD) and caffeic acid O-methyltransferase (COMT), respectively. CAD catalyzes the synthesis of coniferyl and p-coumaryl alcohols, while COMT catalyzes the synthesis of sinapyl alcohol (Halpin *et al.*, 1998; Vignols *et al.*, 1995). The *bm2* gene encodes a functional methylenetetrahydrofolate reductase (MTHFR) involved in the formation of the critical methyl donor, S-adenosyl-L-methionine (SAM) (Tang *et al.*, 2014). SAM links MTHFR with lignin biosynthesis by serving as a methyl donor for both COMT and caffeoyl CoA 3-O-methyltransferase (Tang *et al.*, 2014). The *bm4* gene encodes a functional folylpolyglutamate synthase (FPGS, EC# 6.3.2.17) that acts upstream of MTHFR in the lignin biosynthetic pathway (Li *et al.* 2015). Using a series of allelic crosses of uncharacterized bm mutations with a known set of bm mutations, Ali and co-workers (2010) identified two new additional brown midrib mutations, *bm5* and *bm6*. The *bm5* mutation was identified as 4-coumarate coenzyme A ligase1 (4CL1), affecting G lignin biosynthesis and soluble feruloyl derivatives accumulation in lignified maize tissues (Xiong *et al.*, 2019). Chen and co-workers (2012) characterized the *bm6* mutation for plant height, cell wall digestibility and fine mapped the locus to a 180 kb chromosomal region on the short arm of chromosome 2 but did not identify the underlying gene.

This study identified a candidate *Bm6* gene via a map-based cloning approach. The candidate gene was validated by independent analyses of the *bm6-ref* and an exonic *Mutator* transposon insertional allele, *bm6-P48F9*. The RT-PCR expression analysis further confirmed the presence of the Mutator transposon in intron2 and exon2 in the *bm6-ref* and *bm6-P48F9* alleles, respectively, resulting in significant changes in gene expression of Zm00001d001959 in mutants as compared to their wild-type sibs. The *bm6* locus encodes for a functional GTP Cyclohydrolase1 (GCH1) and illustrates a role for GCH1 in the tetrahydrofolate biosynthetic process.

Table 2 - List of genes in the *bm6* fine-mapped interval on maize chromosome 2 (Public_B73v4) and their expression profile.

Gene ID_v4	Genomic Location	Gene Annotation	Gene Expression
Zm00001d001948	2: 3,416,796 - 3,418,004	Homeobox-TF 67; hb67	Leaves, anther, ear
Zm00001d001949	2: 3,418,932 - 3,422,178	Ubiquitin-like super family protein	Tassel, ear, base of stage 2 leaf (v7), 4th internode
Zm00001d001951	2: 3,423,831 - 3,424,283	PHD finger-like domain-containing protein 5A	Tassel, ear, 4th internode, embryo, 6DAP seed
Zm00001d001952	2: 3,425,808 - 3,432,915	Zinc finger C-x8-C-x5-C-x3-H typefamily protein	Roots, leaves, ear, embryo, anther, 4th internode
Zm00001d001953	2: 3,438,958 - 3,444,350	IQ calmodulin-binding motif family protein	Tassels, silk, base of stage 2 leaf (v7), brace roots
Zm00001d001959	2: 3,543,770 - 3,549,932	GTP cyclohydrolase1	Roots, leaves, germinating kernels, embryo
Zm00001d001960	2: 3,559,183 - 3,560,951	fht1 - Flavanone 3-hydroxylase1 (F3H)	Tassel, weak in leaves and anthers
Zm00001d001961	2: 3,566,924 - 3,567,634	Uncharacterized; provisional gene set	Endosperm, 18DAP seed

Material and methods

Materials

The *bm6* mutant stock 209C (derived from stock 5803 J bm*-86-87-8875-6; designated here as *bm6-ref*; Fig. 1A) was acquired from the Maize Genetics Center and used in crosses with two non-stiff stalk (NSS) Corteva Agriscience elite inbred lines to generate two F2 populations. Three germinal *Mutator* insertions, P03 48 F-09 (referred as *bm6-P48F9*, Fig.1B), PV03 27 H-12, and PV03 5 G-05, were identified using the Corteva Agriscience Trait Utility System for Corn (TUSC). These three TUSC alleles were crossed to an NSS Corteva Agriscience elite inbred line to develop F2 populations.

Fine Mapping of the bm6-ref allele

The segregating F2 plants from each population of the *bm6-ref* allele were scored for the brown midrib phenotype and genotyped using 20 SNP markers corresponding to the region identified by Chen and coworkers (2012) on the short arm of maize chromosome 2. After confirming the *bm6* locus map position, 2944 F2 kernels were seed-chipped and genotyped using 4 flanking polymorphic TaqMan markers (Applied Biosystems, CA). Selected kernels showing recombination breakpoints in the *bm6* region were planted in the field, characterized for the brown midrib and wildtype phenotypes, and genotyped again using the same TaqMan markers. Additional markers were developed *in-house* based on 56K array data and other previously identified SNPs. Briefly, marker sequences were put into the

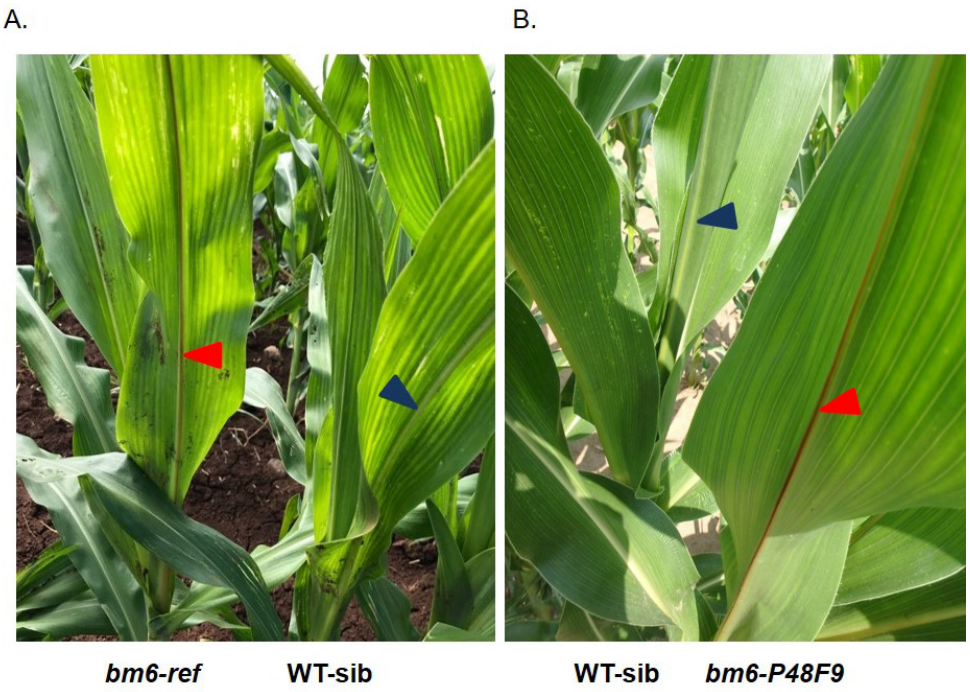

Fig. 1 - Phenotypic characterization of the *brown midrib6 (bm6)* mutation. *bm6* mutants display reddish-brown pigmented leaf midribs (red arrows) versus green midribs in their wild-type sibs (blue arrows). A - The *bm6-ref* allele introgressed into a Corteva Agriscience non-stiff stalk (NSS) inbred line at the V6 growth stage. B - The *bm6-P48F9* mutant segregating in F2 population of a cross between a Corteva Agriscience NSS inbred line and the *bm6-P48F9* TUSC mutant allele at the V7 growth stage.

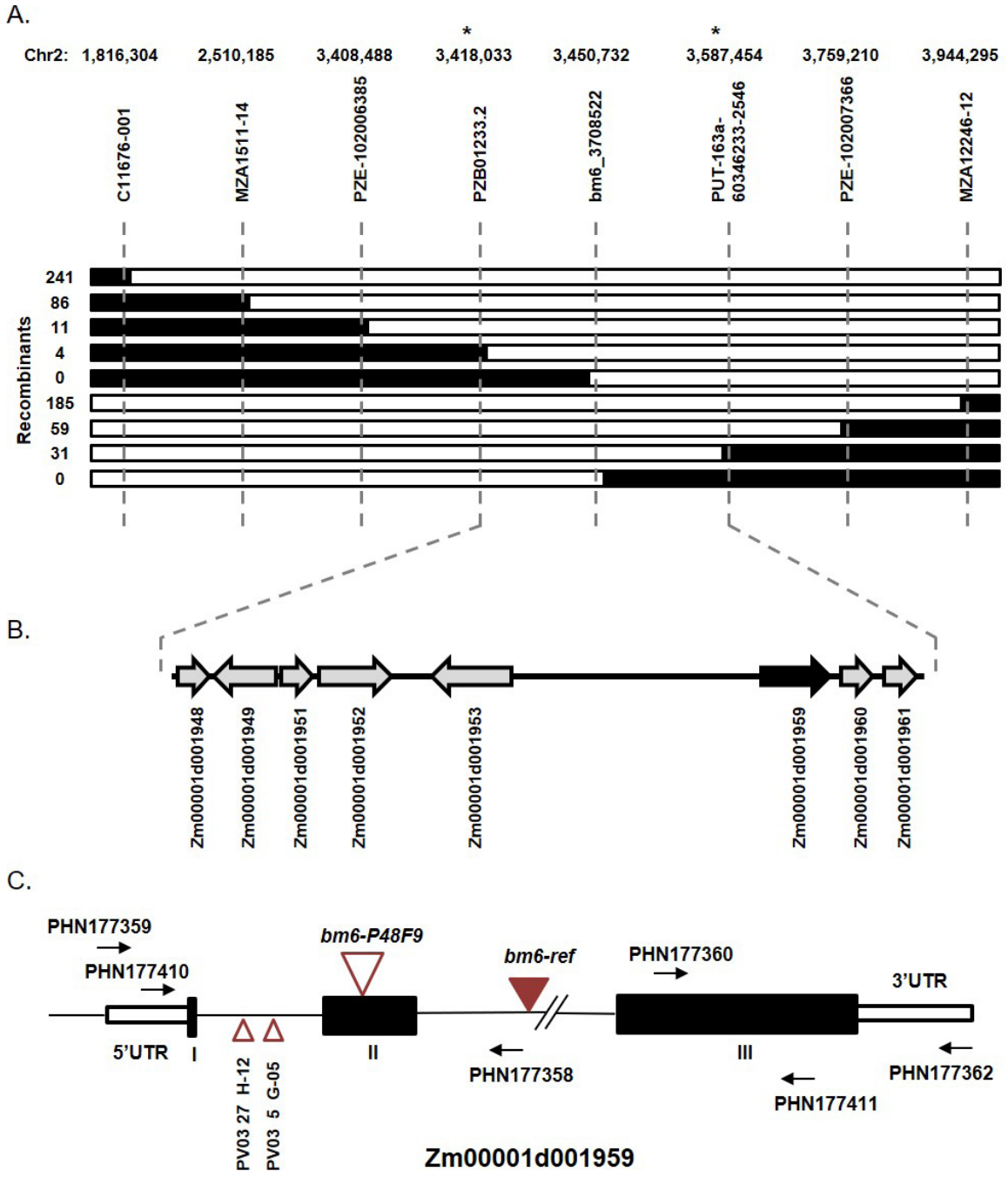

Fig. 2 - *Bm6* candidate gene identification. A – Map-based cloning of the *bm6-ref* allele. Chromosomal regions ruled out by the recombination breakpoints are indicated by black bars. The number of plants listed on the lefthand side for each recombinant class. Asterisks indicate diagnostic markers flanking the fine-mapped interval. B - Eight genes were detected in the fine-mapped interval and each filled arrow represented their directions. The Zm00001d001959 (dark black arrow) was identified as a putative candidate gene for the *Bm6* locus. C - The gene structure of Zm00001d001959. The *Bm6* gene consists of three exons (filled rectangles), two introns (thin lines), and 5' and 3' untranslated regions (empty rectangles). The *bm6-ref* allele has a *Mutator* (*Mu*) insertion in intron 2 (red triangle). TUSC analysis identified three germinal *Mu*-insertions (empty triangles). One of these three insertions had an insertion site in exon2, which is causative for the *bm6-P48F9* allele. PHN numbers and arrows denote gene-specific primers used for PCR fingerprinting and RT-PCR expression and for their directions, respectively.

Primer Picker tool from LGC Biosearch Technologies to design primers (LGC Biosearch Technologies, CA) for the Kompetitive allele-specific PCR (KASP) genotyping assays. Markers polymorphic using genomic DNA (gDNA) extracted from *bm6-ref* homozygotes, the wild-type parent inbred line, and plants heterozygous across the fine-mapped region were selected. The selected markers were then run on the recombinant plants grown in the field to narrow the interval as much as possible. Table 1 lists the KASP markers used to narrow down the chromosomal region associated with the *bm6 locus*.

Candidate Gene Identification

Based on annotation and expression of the genes within the fine-mapped interval, a putative candidate for the *bm6* mutation was selected. Nested PCR primers were designed based on the public domain genomic sequence. PCR amplification of the *bm6* mutant and its WT sib, using GoTaq (Promega (Promega, WI), generated nested fragments to overcome difficulties in amplifying this region. Initial-round PCR amplification utilized outer primers, and then the initial PCR product diluted 1:50 (v/v) and used as a template with inner nested primers.

Candidate Gene Validation for the bm6 mutation

Gene-specific primers (GSPs) from the *bm6* candidate gene was combined with a *Mu*-TIR primer to establish a tight linkage between the candidate gene and the *bm6* mutant phenotype. The BC3F3 mapping consisted of genomic DNA of 24 homozygous *bm6-ref* mutants and 24 homozygous WT sibs (+/+). PCR used two GSPs (PHN177359 and PHN177358) and a primer designed from the *Mutator*-Terminal Inverted Repeat (*Mu*-TIR; PHN9242). The PCR products were excised from the gel, cloned in a TA cloning vector and sequenced using M13F (5′-GTAAAACGACGGCCAGT-3′) and M13R (5′-CAGGAAACAGCTATGAC-3′) primers. In addition, genomic DNA from seven transposon-induced *Mu*-insertion alleles, identified using TUSC, were amplified using the same parameters as above.

RNA Isolation and RT-PCR

For reverse transcriptase-polymerase chain reaction (RT-PCR), the leaf samples from 4-5 weeks old plants grown in the field were collected when the *bm6* phenotype appeared. The total RNA was isolated using the RNeasy plant mini kit (Qiagen, MD). According to the manufacturer's instructions, first-strand cDNA synthesis used a QuantiTec reverse transcription kit (Qiagen, MD). *ZmActin1*, amplified with *ZmActin1*-F (5′-CTGACGAGGATATCCAGCCTATCGTATGTGA-CAATG-3') and *ZmActin1*-R (5′-AACCGTGTGGCTCA-CACCATCACC-3') primers, as internal control, and then GSPs from maize were used to amplify transcripts of *bm6*-ref and *bm6-P48F9* and their WT sibs. RT-PCR reaction included GSPs and two microliters of the reverse transcription reaction products. The RT-PCR program consisted of 95°C for 2 min, 35 cycles of 95°C for 15 sec, 64°C for 15 sec, 72°C for 30 sec, and final extension at 72°C for 7 min in a 25-uL volume.

Sequence analysis

The LASERGENE® bioinformatics computing suite MEGALIGN® program (DNASTAR® Inc., WI) and BioEdit (Hall, 1999) computed the Sequence alignments and percent identity calculations. Multiple sequences alignments used the ClustalW alignment method (Higgins and Sharp, 1989) with the default parameters (GAP PENALTY=l0, GAP LENGTH PENALTY=l0). The Geneious Prime Clustal alignment tool (Biomatters Inc., NZ) created the sequence alignment figures. Default parameters for pairwise 60 alignments using the ClustalW method were KTUPLE=1, GAP PENALTY=3, WINDOW=5, and DIAGONALS SAVED=5).

Cloning and Sequencing of RT-PCR Transcripts

The RT-PCR transcripts from the bm6-ref and bm6-P48F9 alleles, along with their WT sibs, were excised from the gel, purified, and cloned using the TOPO TA Cloning Kit for Sequencing (Invitrogen, CA) according to the manufacturer's instructions. In the case of the bm6-ref allele, all transcripts were excised and purified as a pool. Cloned bands were transformed into Mix & Go! DH5 Alpha Competent Cells (Zymo) using the manufacturer's Mix & Go Transformation protocol. For sequencing, 64 colonies from the bm6-ref allele library, 16 from the *bm6-P48F9* allele, and eight from their WT sibs were selected, and overnight cultures were grown. Plasmid DNA, extracted using the QIAprep Spin Miniprep Kit (Qiagen, MD), was sequenced using M13-Forward and M13-Reverse primers and sequenced using Sequencher 4.8 (Gene Codes Corporation, MI).

Expression Analysis of the bm6 Gene

Profile expression of the maize bm6 gene involved using more than 800 libraries developed by Corteva Agriscience from various tissues collected at different developmental stages and under different biotic and abiotic stress treatments. The average gene expression of Zm00001d001959 was determined using Solexa-WgT (all values in part per ten million or PPTM) and was confirmed using both the eFP Atlas Browser and the RNA-seq expression data from the MaizeGDB public database (*https://www.maizegdb.org/gene_center/gene/Zm00001d001959*).

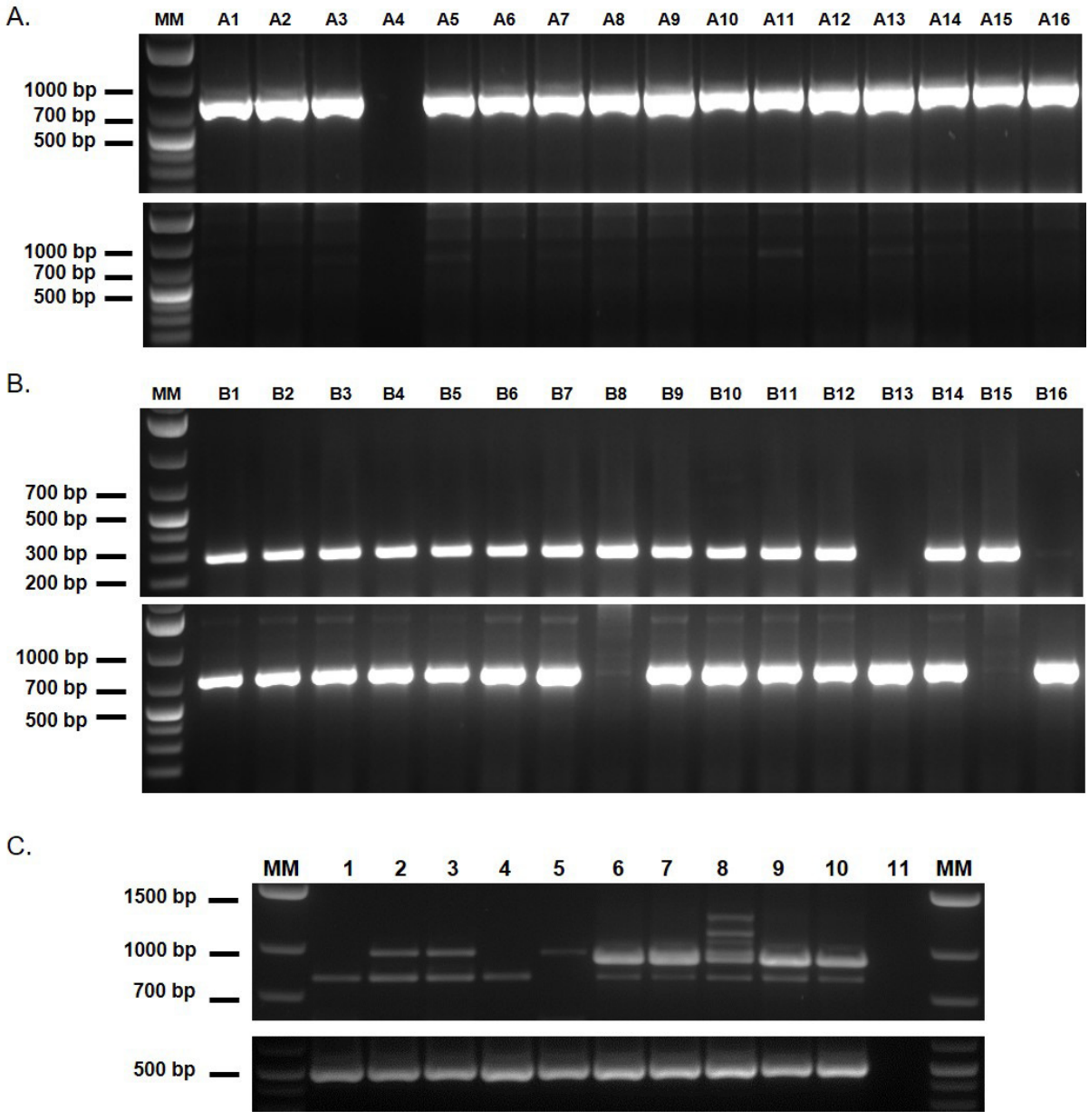

Fig. 3 - Genotyping and expression analysis of the *bm6-ref* and *bm6-P48F9* alleles. A - Gene- specific primer (GSP), PHN17739, in combination with a *Mu-TIR* primer (PHN9242) amplified a ~750 bp PCR products (upper panel, lane A4 missing sample). Two GSPs (PHN177359 and PHN177358) flanking the *Mu*-insertion site in the *bm6-ref* allele were unable to amplify any product in all plants tested (lower panel) indicating that all bm6-ref plants tested were homozygous mutants. B - Similarly, the PCR-fingerprinting of segregating F2 plants, using the same set of primers as in Fig. 3A, identified two plants (# B8 and B15) homozygous for the *bm6-P48F9* insertional allele, and two plants (B13 and B16) homozygous for wildtype allele. The rest of the 12 plants were heterozygotes for the *bm6-P48F9* insertional allele. C - The RT-PCR expression analysis of the *bm6* alleles. The *bm6-P48F9* allele either contains a larger transcript (lanes 2, 3, and 5, upper panel) or missing transcript (lanes 1 and 4, upper panel) to its contrasting wild-type sib (lane 6). The *bm6-ref* allele detected multiple species of mRNA of variable sizes (lane 8) as compared to a small size transcript in its wild-type sib (lane7) and recurrent inbred parents (lanes 9 and 10). RT-PCR controls are distilled water in lane 11, and *ZmActin1* in the lower panel.

Results and discussion

Fine mapping of the Bm6 locus

Since Chen and co-workers (2012) previously mapped the *bm6-ref* mutation to the short arm of chromosome 2 (Chen *et al.*, 2012), 75 segregating F2s plants from each of the two *bm6-ref* mapping populations were screened with 20 Corteva Agriscience maize proprietary markers to confirm the *bm6-ref* map location. These markers covered a 25cM interval between 0 - 25.19cM on the short arm of chromosome 2. Next, 2944 F2 kernels (30 x 96 well plates) from one segregating population were processed for kernel-chipping and genotyped using 8 TaqMan markers to identify 556 recombinants representing 21 different combinations of 4 polymorphic markers covering the 11.69cM to 25.19cM region. Recombinants, along with the homozygous *bm6-ref* mutant, inbred parent, and F1s, were planted in the field, genotyped, and characterized for their phenotypes. Out of 556 recombinant lines, we identified 146 lines segregating for the *bm6-ref* allele and 410 for the WT sib allele. This segregation pattern fits a 1:3 ratio, implying that the *bm6-ref* allele is a single recessive locus ($\chi 2 = 0.470$). Marker data analysis placed the *bm6* locus to a 2.1cM interval on chromosome 2, between physical map positions 1,816,304 -3,944,295 on the Public_B73v4 maize genetic map. The recombination frequency using *in-house* developed KASP markers further delimited the position of the *bm6* to a 169. 4 kb interval between physical map positions 3,418,033 - 3,587,454 (Fig. 2). The two flanking markers, PZB01233.2 and PUT-163a-60346233-2546 (marked with asterisks in Fig. 2A), delimited 4 and 31 recombinants, respectively. The KASP marker bm6_3708522, situated between the two flanking markers at physical position 3,450,732, co-segregates with the *bm6* phenotype.

Identification of a candidate gene for the bm6 mutation

The physical distance in between the bm6_3708522 and a left-flanking marker, PZB01233.2 (Zm-B73-REFERENCE-GRAMENE-4.0), is ~32.7 kb, and this region harbored five genes; Zm00001d001948, Zm00001d001949, Zm00001d001951, Zm00001d001952, and Zm00001d001953. In contrast, the bm6_3708522 marker is ~136.7 kb from the right-flanking flanking marker PUT-163a-60346233-2546, and only three genes; Zm00001d001959, Zm00001d001960, and Zm00001d001961, were detected within this interval. Thus, the 169.4 kb fine-mapped interval contains eight genes (Fig. 2B). Table 2 lists the gene annotations and expression profiles of these eight genes. We considered Zm00001d001959 the best putative candidate gene responsible for the *bm6* phenotype based on its location (2: 3,543,770 - 3,549,932), physically situated next to the KASP marker bm6_3708522 (2: 3,450,732), and its annotation. Zm00001d001959 is annotated as a *Guanosine triphosphate (GTP) cyclohydolase1* in maize *(ZmGch1)* and is a homolog of Arabidopsis *GTP cyclohydrolase1* (AT3G072270.1; GCH1). The alignment of the full-length EST sequence with the genomic sequence from MaizeGDB confirmed that the Zm00001d0001959 gene consists of three exons and two introns (Fig. 2C). Exon1 is only one bp long, whereas exon2 and exon3 are 246 bp and 1184 bp long, respectively. Intron1 is 124 bp long, whereas the intron2 is 4140 bp in size. Next, genomic DNA (gDNA) of homozygous *bm6-ref* and homozygous wild-type sibs (WT sib) was used to PCR-amplify the entire Zm00001d001959 gene from both *bm6-ref* mutant and its WT sib using GSPs designed from the genomic sequence of *ZmGch1* (*Table S1*). The lack of PCR amplification for the region between the end of exon2 and first 300 bp of intron2 in the *bm6-ref* allele using PHN177359 and PHN177358 GSPs suggested a structural change in comparison to the WT sib. Since the *bm6-ref* allele was isolated from *Mu*-active materials (5803J bm*-86-87-8875-6; wx1-Mum6 stock), we amplified the *bm6-ref* material using a combination of the GSP (PHN177359) and a *Mutator*-Terminal Inverted Repeat (*Mu*-TIR) primer to determine if a *Mutator* transposon insertion was present. The primer combination amplified a ~750 bp PCR product in all plants containing the *bm6-ref* allele (Fig. 3A, upper panel). No PCR product was amplified from *bm6-ref* plants using two GSPs flanking the insertion, indicating that all *bm6-ref* plants were homozygous for the *bm6-ref* allele (Fig. 3A, lower panel). The cloning and sequencing of the PCR products confirmed the presence of a *Mu*-insertion in intron2, ~181 bp downstream from the exon2-intron2 junction of the candidate gene. In a population of 118 BC1F2 plants, all individuals containing the *Mu* insertion in Zm00001d001959 exhibited the *bm6* phenotype, indicating that the *Mu* insertion causes the *bm6* phenotype.

Transcript analysis of the bm6-ref allele

The *Mu*-insertion in the *bm6-ref* allele resulted in six alternate mRNAs species (larger sizes) with variable expression levels in RT-PCR analysis as compared to one smaller size transcript in its WT sib (Fig.3C). Cloning and sequencing analysis of all six mature transcripts of the *bm6-ref* allele along with the one transcript of its WT sib revealed that five of the six mature transcripts of the *bm6-ref* allele retained 124 bp sequence of intron1 as compared to functional cDNA of its WT sib (Fig.4). Similarly, in five of the six mature transcripts, a part of

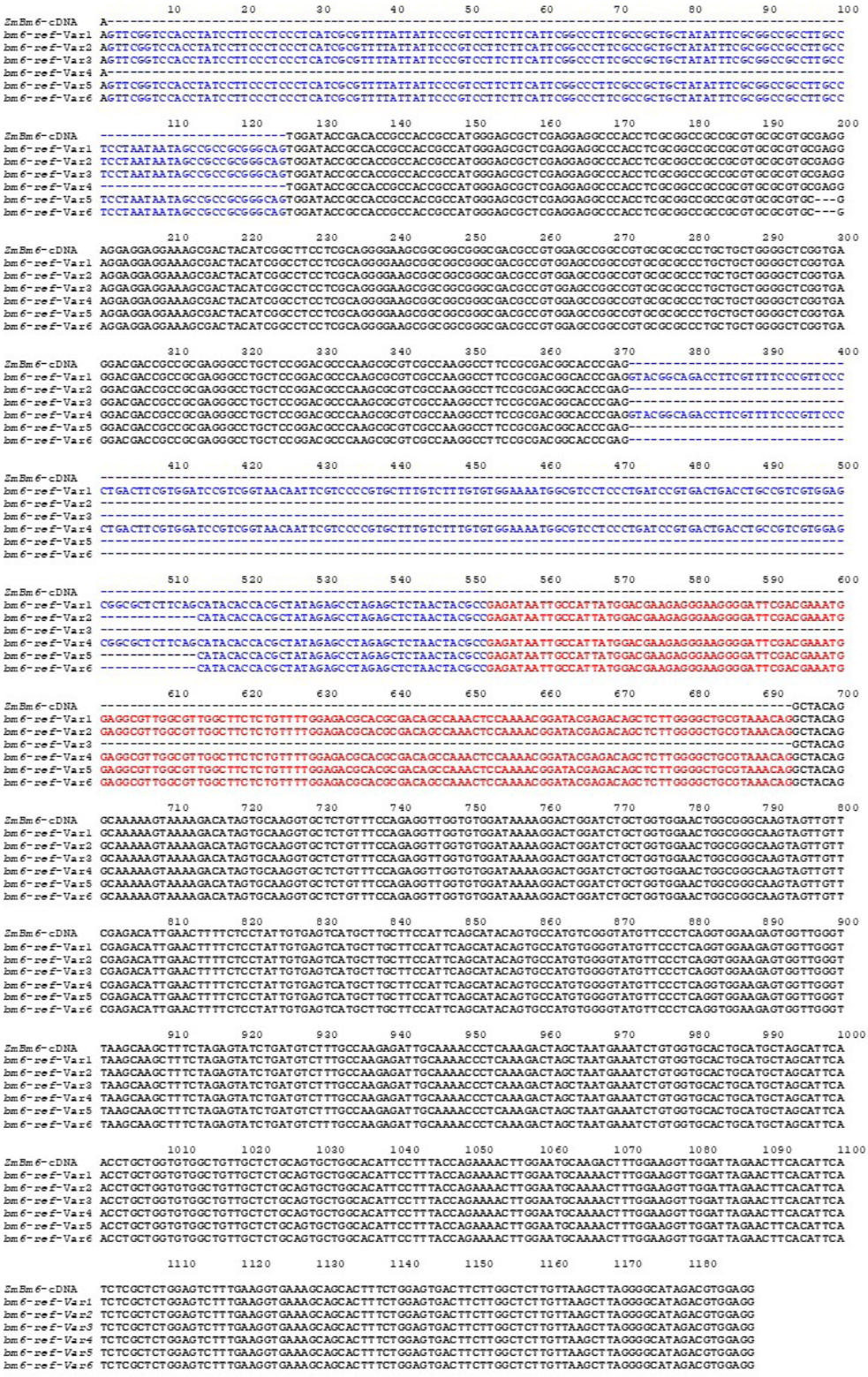

Fig. 4 - A multiple alignments of six *bm6-ref* allele mature transcripts (designated here *bm6- ref*-var1 to *bm6-ref*-var6) and a functional wild-type sib transcript (*ZmBm6*-cDNA) amplified by RT-PCR (Fig. 3C). Bold black letters represent exons 1, 2, and 3, and blue letters represent intronic sequences. Five of the six mature *bm6-ref* allele transcripts contained an additional 141 bp of the *Mutator*-terminal inverted repeat sequence (highlighted in bold red) in intron2

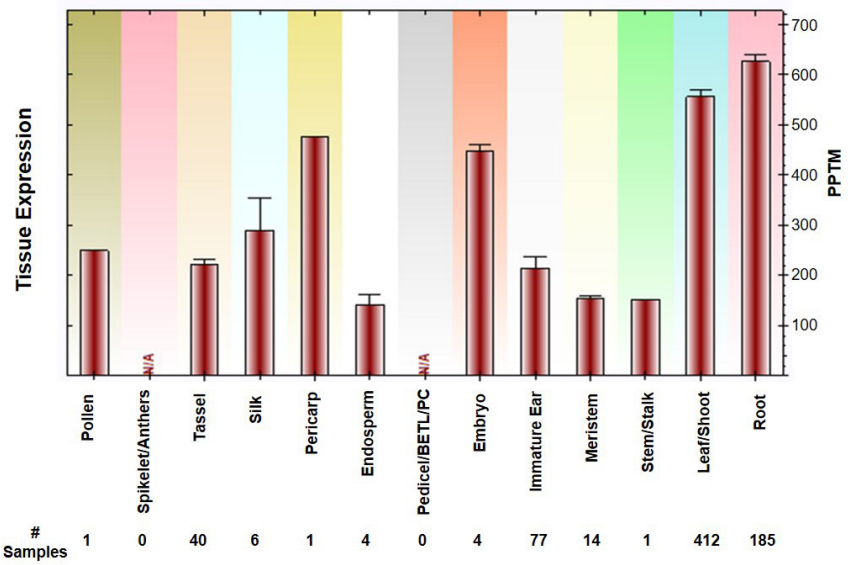

Fig. 5 - The tissue-specific expression of the *Bm6* gene (Zm00001d001959) in B73. Expression was measured in part per ten million (PPTM) using the Solexa-AgT Platform. The number of samples for each tissue is presented at the bottom. The error bars represent the standard error of the mean.

the intron2 (39 bp or 181 bp) and 141 bp of *Mu*-TIR sequences were detected (Fig.4). A BLAST search using 141 bp of the *Mu*-TIR as a query identified a *Mutator1 (Mu1)* insertion in intron2 of Zm00001d001959 in the *bm6-ref* allele. The mature transcripts of the *bm6-ref*-var5 and *bm6-ref*-var6 also showed a three bp deletion (indel) in the exon2 sequence compared to *bm6-ref*-var1, *bm6-ref*-var2, *bm6-ref*-var3, *bm6-ref*-var4, and the functional *ZmBm6*-cDNA (Fig.4). This three bp deletion in transcripts of two variants belonged to a natural variation of an SSR $(GAG)^3$ compared to $(GAG)^4$ in the other four variants and its WT sib. Since exon 1 of the *ZmGch1* gene is only one bp long, the addition of 124 bp of intron1 in five of the six mature transcripts of *bm6-ref* disrupted the starting codon (ATG). The *Mu1*-insertion in intron2 of the *bm6*-ref allele interfered with splicing and produced multiple species of mature transcripts for the *ZmGch1* gene. The differential splicing of intronic sequences and 141 bp of *Mu*-TIR in all six *bm6-ref* mature transcripts resulted in a frameshift and early termination of their predicted polypeptides leading to a null mutation

Candidate gene validation for the bm6 mutation

To further support that the *bm6* phenotype results from a mutation in *ZmGch1*, we took advantage of the existing TUSC facility in Corteva Agriscience to identify additional *Mutator* transposon insertion alleles (Meeley and Briggs, 1995). Reverse genetics screening of gDNA from ~42,000 F2 plants from the TUSC library identified seven TUSC alleles (*Fig. S1*). The cloning and sequencing of the PCR products of TUSC alleles confirmed that six of the seven TUSC alleles had *Mu*-insertions in introns, four in intron1 and two in intron2, whereas one TUSC allele, PV03 48 F-09, had a *Mu*-insertion in exon2 of Zm00001d001959. Due to low germination rates, only F2 seed of the exon2 insertion P03 48 F-09 and intronic insertions PV03 27 H-12, and PV03 5 G-05 were available for analysis (Fig.2C). Fingerprinting of F2 plants from each of the three alleles confirmed that the *Mu*-insertions were germinal. The lines were maintained by crossing heterozygous TUSC plants with a Corteva Agriscience NSS inbred line. The PHN177359 GSP primer from the 5'UTR of Zm00001d001959 gene in combination with *Mu*-TIR primer (PHN9242) resulted in 300 bp products in homozygous and heterozygous plants of P03 48 F09 allele (Fig. 3B). Most plants analyzed in the P03 48 F09 allele were heterozygous for the insertion, except for two plants homozygous for the mutant allele and two plants homozygous for the wild-type allele (Fig. 3B). The cloning and sequence of the PCR product confirmed a *Mu*-insertion in exon2, 11 bp downstream of the intron1-exon2 junction. The two plants homozygous for the P03 48 F-09 allele showed a brown midrib phenotype, whereas the two intronic alleles, PV03 27 H-12 and PV03 5 G-05, did not segregate for the mutant phenotype in their populations (data not shown). The PV03 48 F-09 allele, designated as *bm6-P48F9*, was also allelic in crosses with the *bm6-ref* allele (Fig. 1B). The extended reverse genetic analysis of 86 plants of the F2 population of the *bm6-P48F9* allele demonstrated a complete linkage between the *Mu*-insertion in exon2 of the *bm6-P48F9* allele and its brown midrib mutant phenotype.

Furthermore, RT-PCR expression analysis of the *bm6-P48F9* allele detected a complete absence of a single larger size transcript than its WT sib and the recurrent inbred parent line (Fig.3C). The sequence analysis of the mature *bm6-P48F9* transcript detected the presence of 149 bp of intron1 and a three bp addition each at two sites in exon2 as compared to the functional wild-type transcript of its WT sib (*Fig S2*). These changes in the *bm6-P48F9* allele led to a frameshift and an early termination of its predicted polypeptide. Thus, a *Mu*-insertion in exon2 of the *bm6-P48F9* allele made it a null mutation, and these results provided independent support that we have isolated the correct gene for the *bm6* locus. Furthermore, these results also suggest that the brown midrib phenotype in both *bm6* alleles might be due to *Mu*-insertion interference leading to the lack of expression of the functional wild-type transcript of the *bm6* gene. A minor transcript amplified in both mutant alleles, their WT sibs, and recurrent inbred parents by RT-PCR using GSPs PHN177410 and PHN177411 was cloned and sequenced (Fig.3C). Its sequences in both mutant alleles and their WT sibs were the same (data not shown) and aligned with Zm00001d026531, a homolog of Zm00001d001959 on chromosome 10, indicating that the homolog might have a different function.

Expression analysis of the ZmGch1

The *bm6* gene is expressed in multiple plant tissues with maximum average expression in roots (650 PPTM) and leaf/shoot (575 PPTM), in 185 and 412 samples, respectively (Fig.5). The maximum average expression is 450 PPTM in embryo and pericarp, 300 PPTM in silk, 200 PPTM in immature ears, and 100 PPTM in meristem samples (Fig.5). The expression profile of Zm00001d001959 was also confirmed using the eFP Atlas Browser (Winter *et al.*, 2007) from MaizeGDB, detecting maximum expression in the primary root (developmental zone, root cortex, and stele), crown roots at 1-5 days old seedlings, first internode (V5), SAM, stem, tassel (V18), post-pollination leaves (0-6 DAP), and pericarp (Hoopes *et al.*, 2019). RNA-seq expression data from MaizeGDB further confirmed that maximum expression of Zm00001d001959 (60.1 FPKM; Fragment read Per Kilobase per Million mapped reads) is in germinating kernels (2 DAI), 58.1 FPKM in the root cortex of 5 days old seedlings, 36.9 FPKM in embryos (38 DAP), 30.6 FPKM in mature leaf (V8), 26.5 FPKM in V7-V8 internodes, and 18.7 FPKM in the meristem of 16-19 days old plants. These results indicate that Zm00001d001959 is expressed in the roots of germinating seedlings and then upregulated in mature leaves, internodes, and meristem tissues. A high Pearson correlation (0.7043) between Zm00001d001959 expression and the expression of the *Folypolyglutamate synthase* (FPGS) gene mapped on chromosome 9 was detected in the Solexa WgT database of the Corteva Agriscience indicating the functional role of *GTP1 cyclohydrolase1* in the tetrahydrofolate (THF) biosynthesis II pathway. FPGS plays multiple roles in plants. The maize *bm4* gene encodes a functional *folypolyglutamate synthase* (Li *et al.*, 2015), which is involved in the poly-glutamylation of THF as a part of one-carbon (C1) metabolism (Cossins and Chen, 1997; Mehrshahi *et al.*, 2010).

The bm6 candidate gene is a GTP cyclohydrolase1 (GCH1)

The Zm00001d001959 gene is a homolog of Arabidopsis AT3G07270, annotated as *GTP cyclohydrolase1* (source: Araport11). The *GTP cyclohydrolae1* is involved in 7,8-dihydroneopterin 3'-triphosphate, tetrahydrobiopterin, and tetrahydrofolate biosynthesis. GTP cyclohydrolase1 (GCH1) mediates the first and committing step of the pterin branch of the 6-hydroxymethyl-dihydropterin diphosphate biosynthesis I (*https://pmn.plantcyc.org/ARA/NEW-IMAGE?object=PWY-6147*). Based on the Gene Ontology provided by TAIR (The Arabidopsis Information Resource), this peptide is involved in tetrahydrofolate biosynthesis (*https://pmn.plantcyc.org/ARA/NEW-IMAGE?object=PWY-3742*). Tetrahydrofolate (vitamin B9) and its derivatives, commonly termed folates, are vital cofactors for enzymes mediating one-carbon-transfer reactions (Cossins and Chen, 1997; and Hanson *et al.*, 2000). Folates are involved in a wide range of critical metabolic functions, including the biosynthesis of methionine, purines, thymidylate, and pantothenate. In plants, folates are also involved in photorespiration, amino acid metabolism, and chloroplastic protein biosynthesis (Hanson and Gregory, 2002; Jabrin *et al.*, 2003). The fluxes through C1 pathways mediated by folates are exceptionally high for methylated compounds such as the secondary metabolites lignin, alkaloids, betaines, and primary metabolites such as choline, pectin, and chlorophyll (Hanson and Roje, 2001). The BLASTP search at NCBI revealed two identifiable conserved domains, GTP cyclohydrolase1 domain (IPR043134) and NADPH-dependent 7-cyano-7-deazaguanine reductase (IPR043133) in the ZmGCH1 polypeptide. The ZmGCH1 polypeptide is 476 amino acids (aa) long compared to 466 aa in Arabidopsis and 478 aa in sorghum. The deduced amino acid sequence of the maize GCH1 polypeptide was aligned with homologous polypeptides of both monocot and dicot plant species and presented in Figure 6. Among monocots, the GCH1 polypeptides of sorghum, foxtail millet (*Setaria italica*), and rice (*Oryza sativa*) were 92.9%, 88.9%, and 82.4% identical with maize at amino acid

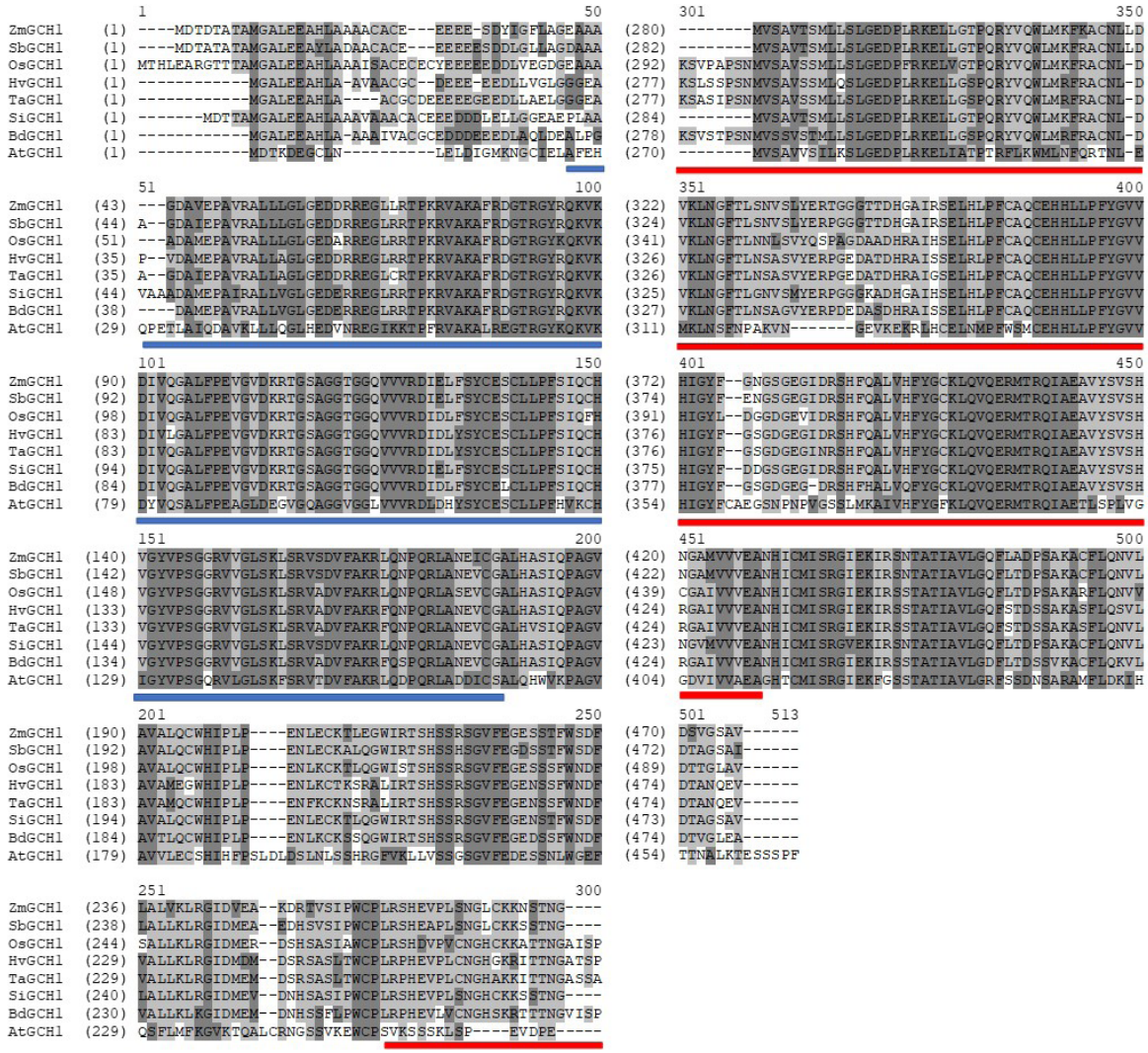

Fig. 6 - Multiple alignments of the predicted polypeptide of maize GTP cyclohydrolase1 (ZmGCH1) with that of sorghum (SbGCH1), rice (OsGCH1), barley (HvGCH1), wheat (TaGCH1), foxtail millet (SiGCH1), Brachypodium (BdGCH1), and Arabidopsis (AtGCH1). Two highly conserved domains, IPR043134 (156 amino acids long GTP cyclohydrolase1 domain starting from 39 to 190 amino acids) at the N-terminal end (underlined by a blue bar), and IPR043133 (186 amino acids long GTP cyclohydrolase I/NADPH-dependent 7-cyano-7- deazaguanine reductase domain starting from 274 to 459 amino acids) at the C-terminal end (underlined by a red bar) are present in all plant species.

level, respectively, in contrast to the barley (*Hordeum vulgare*), wheat (*Triticum aestivum*), and *Brachypodium distachyon* polypeptides have diverged from maize and showed only 78%, 77.3%, and 79.0% identity, respectively. Homologs in dicots, including Arabidopsis (*Arabidopsis thaliana*) and soybean (*Glycine max*), showed 49.4% and 49.6% identity with the ZmGCH1 polypeptide at the global alignment level, respectively. The multiple alignments also confirmed that two domains of the GCH1 polypeptides are highly conserved in all plant species (Fig. 6). The first GTP cyclohydrolase1 domain, IPR043134, is 156 aa long at N-terminal, and the second GTP cyclohydrolase1 /NADPH-dependent 7-cyano-7-deazaguanine reductase domain, IPR043133, is 186 aa long at C-terminal.

Potential use of Gch1 locus in Sorghum

The quality and advantages of sorghums with the brown midrib (BMR) gene are now well established, and BMR forages can equal the feeding value of corn silage at significantly lower water and input requirements as well as much lower seed costs (McCollum *et al.*, 2010). The *bmr6* and *bmr12* mutants are *loss-of-function* mutations in sorghum genes orthologs of *bm1* (CAD) and *bm3* (COMT) of maize, respectively, and are being used commercially for silage (Sattler *et al.* 2010; Saballos *et al.*, 2012). The highest global identity of SbGCH1 polypeptide is that of the maize GCH1 polypeptide, suggesting the conservation of function of GCH1 in sorghum and its loss-of-function mutation

in sorghum could offer potential use as silage. Furthermore, a non-GMO brachytic dwarf, photoperiod sensitive, and male-sterile forage sorghum BMR 60D hybrids offered by sorghum seed industries might be ideal for delivering a much higher leaf to stalk ratio for improved feed quality and palatability in Europe (McCollum *et al.*, 2010).

Conclusions

In the present investigation, we confirmed mapping and fine-mapping results earlier reported by Chen and co-workers using the same *bm6-ref* allele (Chen *et al.*, 2012) and identified a candidate gene for *Bm6* by a map-based cloning approach. A loss-of-function mutation caused by the insertion of *Mu1* in intron2 of GTP *Cyclohydrolase1 (Gch1)* was responsible for the *bm6-ref* mutant phenotype. Isolation of additional alleles using reverse genetics and expression analysis validated the candidate gene for *Bm6. ZmGch1* mediates the first step in the tetrahydrofolate (THF) biosynthetic process and acts upstream of the *bm4* locus, encoding *Folypolyglutamate synthase* (FPGS) in the THF pathway. These results complete the characterization of the last known *brown* midrib mutant in maize and enhance the knowledge for its potential use in maize and sorghum.

Funding

This work was fully supported by Corteva Agriscience

Author Contributions

A.L. Identified a candidate gene for the *bm6-ref* mutation by map-based approach and isolated a causative insertion for the *bm6-ref* phenotype. S.J. Completed PCR-fingerprinting and RT-PCR expression analysis of both the *bm6-ref* and *bm6-P48F9* alleles to validate the candidate gene; L. H. Managed field nurseries and genotyping resources; T.H. Identified TUSC alleles using the Zm00001d001959 genomic sequence; R.B.M. provided resources for TUSC screening, and guidance for this research project; J.J. Identified recombinants for *bm6-ref* allele using seed-chipping and field nursery; K.D.S. Acquired germplasm, managed field nurseries, and assisted in manuscript preparation; D.S.M. Candidate gene isolation and validation, supervised both S.J. and T.H., data analysis, and prepared this manuscript.

Acknowledgement

We are extremely thankful to the members of the Johnston, IA, and Waimea, HI Corteva Agriscience Integrated Field Science group for their invaluable assistance on this project.

Accession Numbers

Maize Acc. No. ONM12562.1 (Zm00001d001959); sorghum Acc. No. XP_021319088.1 (SORBI_3006G254100); rice Acc. No. KAF2936351.1 (Os04g0662700); barley Acc. No. KAE8801101.1 (HORVU2Hr1G109980); wheat Acc. No. ABM54074.1 (TraesCSB02G521000); Brachypodium Acc. No. XP_003580753.1 (BRADI5G25070); Setaria Acc. No. XP_004960185.1 (Si021939m.g); and Arabidopsis Acc. No. NM_111607 (AT3G07270.2).

References

Ali F, Scott P, Bakht J, Chen Y, Lübberstedt T, 2010. Identification of novel brown midrib genes in maize by tests of allelism. Plant Breed 129: 724-726 https://doi.org/10.1111/j.1439-0523.2010.01791.x

Andrieu J, Demarquilly C, Dardenne P, Barrière Y, Lila M, Maupetit P, Rivière F, Femenias N, 1993. Composition and nutritive value of whole maize plants fed fresh to sheep. I. Factors of variation. Ann Zootech 42: 221-249 https://doi.org/10.1051/animres:19930301

Barrière Y, 2017. Brown-midrib genes in maize and their efficiency in dairy cow feeding. Perspectives for breeding improved silage maize targeting gene modifications in the monolignol and p-hydroxycinnamate pathways. Maydica 62: 1-19 https://hal.archives-ouvertes.fr/hal-01595409

Barrière Y, Alber D, Dolstra O, Lapierre C, Motto M, Ordas A, van Waes J, Vlasminkel L, Welcker C, Monod JP, 2005. Past and prospects of forage maize breeding in Europe. I. The grass cell wall as a basis of genetic variation and future improvements in feeding value. Maydica 50: 259-274 http://hdl.handle.net/10261/42856

Barrière Y, Emile JC, Surault F, 2003. Genetic variation of silage maize ingestibility in dairy cattle. Animal Res 52: 489-500 https://doi.org/10.1051/animres:2003042

Barrière Y, Emile JC, Traineau R, Surault F, Briand M, Gallais A, 2004a. Genetic variation for organic matter and cell wall digestibility in silage maize. Lessons from a 34-year long experiment with sheep in digestibility crates. Maydica 49: 115-126 https://hal.inrae.fr/hal-02682464

Barrière Y, Ralph J, Méchin V, Guillaumie S, Grabber JH, Argillier O, Chabbert B, Lapierre C, 2004b. Genetic and molecular basis of grass cell wall biosynthesis and degradability. II. Lessons from brown-midrib mutants. CR Biologie 327: 847-860 https://doi.org/10.1016/j.crvi.2004.05.010

Barrière Y, Riboulet C, Méchin V, Maltese S,

Pichon M, Cardinal AJ, Lapierre C, Lübberstedt T, Martinant JP, 2007. Genetics and genomics of lignification in grass cell walls based on maize as a model system. Genes, Genomes and Genomics 1: 133–156

Baucher M, Monties B, Van Montagu M, Boerjan W, 1998. Biosynthesis and genetic engineering of lignin. Critical Reviews in Plant Sci 17: 125-197 https://doi.org/10.1080/07352689891304203

Boerjan W, Ralph J, Baucher M, 2003. Lignin biosynthesis. Ann Rev of Plant Biol 54: 519-546 https://doi.org/10.1146/annurev.arplant.54.031902.134938

Chen Y, Liu H, Ali F, M. Scott P, Ji Q, Frei UK, Lübberstedt T, 2012. Genetic and physical fine mapping of the novel brown midrib gene *bm6* in maize (*Zea mays* L.) to a 180 kb region on chromosome 2. Theor Appl Genet 125: 1223-1235 https://doi.org/10.1007/s00122-012-1908-5

Cherney JH, Cherney DJR, Akin DE, Axtell JD, 1991. Potential of brown-midrib, low-lignin mutants for improving forage quality. Adv Agron 46: 157-195 https://doi.org/10.1016/S0065-2113(08)60580-5

Cossins EA, Chen L, 1997. Folates and one-carbon metabolism in plants and fungi. Review Phytochemistry 45(3): 437-52 https://doi.org/10.1016/s0031-9422(96)00833-3

Grabber JH, Mertens DR, Kim H, Funk C, Lu F, Ralph J, 2009. Cell wall fermentation kinetics are impacted more by lignin content and ferulate cross-linking than by lignin composition. J Sci Food Agric 89(1): 122-129 https://doi.org/10.1002/jsfa.3418

Grabber JH, Ralph J, Lapierre C, Barrière Y, 2004. Genetic and molecular basis of grass cell-wall degradability. I. Lignin–cell wall matrix interactions. Comptes Rendus Biologies 327(5): 455-465 https://doi.org/10.1016/j.crvi.2004.02.009

Grand C, Sarni F, Boudet AM, 1985. Inhibition of cinnamyl-alcohol-dehydrogenase activity and lignin synthesis in poplar (*Populus* x *euroamericana* Dode) tissue by two organic compounds. Planta 163: 232-237 https://doi.org/10.1007/bf00393512

Hall TA, 1999. BioEdit: A user-friendly biological sequence alignment editor and analysis program for windows 95/98/NT. Nucleic Acids Symposium Series 41: 95-98

Hanson AD, Gage DA, Shachar-Hill Y, 2000. Plant one-carbon metabolism and its engineering. Trends Plant Sci 5(5): 206-213 https://doi.org/10.1016/s1360-1385(00)01599-5

Hanson AD, Roje S, 2001. One-carbon metabolism in higher plants. Ann Rev Plant Physiol Plant Mol Biol 52: 119-137 https://doi.org/10.1146/annurev.arplant.52.1.119

Hanson AD, Gregory JF, 2002. Synthesis and turnover of folates in plants. Curr Opin Plant Biol 5(3): 244-249 https://doi.org/10.1016/s1369-5266(02)00249-2

Halpin C, Holt K, Chojecki J, Oliver D, Chabbert B, Monties B, Edwards K, Barakate A, Foxon GA, 1998. Brown-midrib maize (*bm1*) - a mutation affecting the cinnamyl alcohol dehydrogenase gene. Plant Journal 14(5): 545-553 https://doi.org/10.1046/j.1365-313x.1998.00153.x

Higgins DG, Sharp PM, 1989. Fast and sensitive multiple sequence alignments on a microcomputer. Comput Appl Biosci 5(2): 151-3 https://doi.org/10.1093/bioinformatics/5.2.151

Hoopes GM, Hamilton JP, Wood JC, Esteban E, Pasha A, Vaillancourt B, Provart NJ, Buell CR, 2019. An updated gene atlas for maize reveals organ-specific and stress-induced genes. Plant J 97(6): 1154-1167 https://doi.org/10.1111/tpj.14184

Jabrin S, Ravanel S, Gambonnet B, Douce R, Rebeille F, 2003. One-carbon metabolism in plants. Regulation of tetrahydrofolate synthesis during germination and seedling development. Plant Physiol 131(3): 1431-1439. https://doi.org/10.1104/pp.016915

Jorgenson LR, 1931. Brown midrib in maize and its lineage relations. J Am Soc Agron 23: 549-557 https://doi.org/10.2134/agronj1931.00021962002300070005x

Lauer JG, 1995. Corn hybrids for silage uses. Wisconsin Crop Manager 2(2): 16-18 http://corn.agronomy.wisc.edu/WCM/W012.aspx

Lauer JG, Coors JG, Flannery PJ, 2001. Forage yield and quality of corn cultivars developed in different eras. Crop Sci 41: 1449-1455 https://doi.org/10.2135/cropsci2001.4151449x

Li L, Hill-Skinner S, Liu S, Beuchle D, Tang HM, Yeh C-T, Nettleton D, Schnable PS, 2015. The maize *brown midrib4* (bm4) gene encodes a functional folylpolyglutamate synthase. The Plant J 81: 493-504 https://doi.org/10.1111/tpj.12745

Lorenz AJ, Coors JG, de Leon N, Wolfrum EJ, Hames BR, Sluiter AD, Weimer PJ, 2009. Characterization, genetic variation, and combining ability of maize traits relevant to the production of cellulosic ethanol. Crop Sci 49(1): 85-98 https://doi.org/10.2135/cropsci2008.06.0306

McCollum T, McCuistion K, Bean B, 2010. Brown Mid-rib and photoperiod-sensitive forage sorghums. The Agriculture Program, The Texas A&M University System, AREC 05-20. http://agrilife.org/amarillo/files/2010/11/brownmidrib.pdf

Meeley B, Briggs S, 1995. Reverse genetics for maize. Maize Gene. Coop Newslett 69: 67-67

Mehrshahi P, Gonzalez-Jorge S, Akhtar TA, Ward JL, Santoyo-Castelazo A, Marcus SE, Lara-Núñez A, Ravanel S, Hawkins ND, Beale MH, Barrett DA, Knox JP, Gregory JF, Hanson AD, Bennett MJ, Dellapenna D, 2010. Functional analysis of folate polyglutamylation and its essential role in plant metabolism and development. Plant J 64: 267-279 *https://doi.org/10.1111/j.1365-313x.2010.04336.x*

Moore KJ, Jung HJ, 2001. Lignin and fiber digestion. J Range. Manage 54: 420-430 *https://repository.arizona.edu/handle/10150/643890*

Riboulet C, Fabre F, Dénoue D, Martinant J, Lefevre B, Barrière Y, 2008. QTL mapping and candidate gene research from lignin content and cell wall digestibility in a top-cross of a flint maize recombinant inbred line progeny harvested at silage stage. Maydica 53: 1–9

Saballos A, Sattler SE, Sanchez E, Foster TP, Xin Z, Kang C, Pedersen JF, Wilfred Vermerris W, 2012. *Brown midrib2* (*Bmr2*) encodes the major 4-coumarate: coenzyme A ligase involved in lignin biosynthesis in sorghum (Sorghum bicolor (L.) Moench). Plant J 70 (5): 818-830 *https://doi.org/10.1111/j.1365-313X.2012.04933.x*

Sattler SE, Funnell-Harris DL, Pedersen JF, 2010. Efficacy of singular and stacked *brown midrib 6* and *12* in the modification of lignocellulose and grain chemistry. J Agric Food Chem 58: 3611-3616 *https://doi.org/10.1021/jf903784j*

Tang HM, Liu S, Hill-Skinner S, Wu W, Reed D, Yeh C-T, Nettleton D, Schnable PS, 2014. The maize *brown midrib2* (*bm2*) gene encodes a methylenetetrahydrofolate reductase that contributes to lignin accumulation. Plant J 77: 380–392 *https://dx.doi.org/10.1111%2Ftpj.12394*

Vignols F, Rlgau J, Torres MA, Capellades M, Puigdomènech P, 1995. The *brown midrib3* (*bm3*) mutation in maize occurs in the gene encoding caffeic acid o-methyltransferase. Plant Cell 7: 407-416 *https://doi.org/10.1105/tpc.7.4.407*

Weng J-K, Chapple C, 2010. The origin and evolution of lignin biosynthesis. New Phytologist 187 (2): 273-285 *https://doi.org/10.1111/j.1469-8137.2010.03327.x*

Winter D, Vinegar B, Nahal H, Ammar R, Wilson GV, Provart NJ, 2007. An "Electronic Fluorescent Pictograph" browser for exploring and analyzing large-scale biological data sets. PLoS One 2 (8): e718 *https://doi.org/10.1371/journal.pone.0000718*

Xiong W, Wu Z, Liu Y, Li Y, Su K, Bai Z, Guo S, Hu Z, Zhang Z, Bao Y, Sun J, Yang G, Fu C, 2019. Mutation of 4-coumarate: coenzyme A ligase 1 gene affects lignin biosynthesis and increases the cell wall digestibility in maize *brown midrib5* mutants. Biotech Biofuels 12: 82 *https://doi.org/10.1186/s13068-019-1421-z*

Supplemental Table S1 - A list of the gene-specific primers (GSPs) designed from an 8276 bp genomic sequence of Zm00001d001959, a candidate gene for the *bm6-ref* mutation. The primers with PHN numbers were used in reverse genetics to identify *Mutator* transposon insertion alleles in the TUSC study. Due to difficulties in amplifying some sequence regions, nested primers (denoted by N letter at the end of the forward or reverse primer name) were designed and used in PCR amplifications. The color-highlighted primers detect polymorphism (absence/presence) between the *bm6-ref* allele and its WT sib, and the "Gene Region" column describes the primer location.

Primer Name	Primer Sequence (5' - 3')	Gene Region
PHN177357	TCCCATGCTACTCTACTCTGGCTGCCG	Upstream of 5'-UTR
bm6_2430_1F	ATGCTACTCTACTCTGGCTGCCG	Upstream of 5'-UTR
bm6_2430_1FN	GCGCCTCAGAAAATGTTACCACG	Upstream of 5'-UTR
PHN177359	GATCCTGATCCAACACACATCTCGAGGC	5'-UTR
PHN178410	ACCCCATCGCTTCGTCGCTA	5'UTR
bm6_2430_2F	TTCGTGGATCCGTCGGTAACAA	Intron2
bm6_2430_2FN	TTCGTCCCCGTGCTTTGTCT	Intron2
bm6_2430_1RN	CCGCTCTATAGCGTGGTGTATGC	Intron2
bm6_2430_1R	CGTTCAAATGACATACGGCGTAG	Intron2
PHN177358	CCATACGCGTTCAAATGACATACGGCG	Intron2
bm6_2430_3F	GGCACTTTACTTGCCACTTAATAGT	Intron2
bm6_2430_3FN	GTTGACTATTTATTATGCCTGACGAC	Intron2
bm6_2430_2RN	TCAGAGGTGCTGATGTTGTGAGC	Intron2
bm6_2430_2R	TTACAGCAACAAAGCAACGCAA	Intron2
bm6_2430_4F	GGGTTTTGTCATTTTGGAATTAATG	Intron2
bm6_2430_4FN	GAATGGGCAAGAACATTGATAAATTT	Intron2
bm6_2430_3RN	CAATTTTAAACACACAAACTTCTGTCTC	Intron2
bm6_2430_3R	GTTTTCAAGTACTTAAAGAAGCAACC	Intron2
bm6_2430_5F	GCAGAGTAGATGAGGTGGTGTTAAG	Intron2
bm6_2430_5FN	GGTCTACAAAAAGACGGCATGCT	Intron2
bm6_2430_4RN	CATGTGCATTTCTACAACACTTATCTG	Intron2
bm6_2430_4R	CATAAATCCAATGCAACATGTGC	Intron2
bm6_2430_6F	TTGTTTATCAAGGTGCAGATCGC	Intron2
bm6_2430_6FN	GAGCCAACTTCGAGTCGAGCCT	Intron2
bm6_2430_5RN	TTTGTATCGCCTCTTAGGATCCC	Intron2
bm6_2430_5R	GGCCTTCTCCTGTCTCTCTTCC	Intron2
bm6_2430_7F	TGTAATTTTGAGCAAACGAGCCA	Intron2
bm6_2430_7FN	TCCAATGTCCAACCTCATTTTGA	Intron2
bm6_2430_6RN	GGAGCAGGACCTATCAGCTTCAA	Intron2
bm6_2430_6R	TTTATTGCTCCCAACGAAGGC	Intron2
bm6_2430_8F	TGAGTCATGCTTGCTTCCATTCA	Exon3
bm6_2430_8FN	GCATACAGTGCCATGTCGGG	Exon3
bm6_2430_7RN	GCAGAGCAACAGCCACACCAG	Exon3
bm6_2430_7R	TGGTAAAGGAATGTGCCAGCACT	Exon3
PHN177360	GCAGCACTTTCTGGAGTGACTTCTTGGC	Exon3
PHN178411	TTAGCCTCCACGTCTATGCCCC	Exon3
bm6_2430_9F	TGTGAACACCATCTTCTGCCCT	Exon3
bm6_2430_9FN	TTGGGTACTTTGGCAATGGAAG	Exon3
bm6_2430_8RN	GCCCCATTGTGCGAAACTGAA	Exon3
bm6_2430_8R	TGCAAATGTGGTTGGCCTCA	Exon3
PHN177362	CGATCGGCGTAACATCAAATTCAACGGT	3'-UTR
bm6_2430_9RN	AAATTGGGATGACAAGAGCATGC	Downstream of 3'-UTR
bm6_2430_9R	CAGGATTCAATTCGAACATCGTG	Downstream of 3'-UTR
PHN177361	GGAACGTCCGAAATACGTGAGCCGTG	Downstream of 3'-UTR

E.

Lane	Pedigree	Selected band (bp)
1.	PV03 05 G-05	250
2.	PV03 27 H-12	225
3.	PV03 43 E-05	225
5.	PV03 48 F-09	300
6.	PV03 49 A-07	225
7.	PV03 69 D-03	225
9.	PV03 89 B-04	225
10.	PV03 94 D-07	700
13.	PV03 94 E-04	700
15.	PV03 191 B-11	275
16.	PV03 191 F-04	225
17.	BT94 16 C-04	250
18.	BT94 76 G-02	225
21.	BT94 78 F-10	250
24.	BT94 174 H-11	225

F.

Lane	Pedigree	Selected band (bp)
1.	PV03 05 G-05	600
3.	PV03 43 E-05	675
5.	PV03 48 F-09	575
6.	PV03 49 A-07	700
7.	PV03 69 D-03	700
8.	PV03 69 F-01	275
9.	PV03 89 B-04	700
10.	PV03 94 D-07	
13.	PV03 94 E-04	200
16.	PV03 191 F-04	725
17.	BT94 16 C-04	650
18.	BT94 76 G-02	625
21.	BT94 78 F-10	575

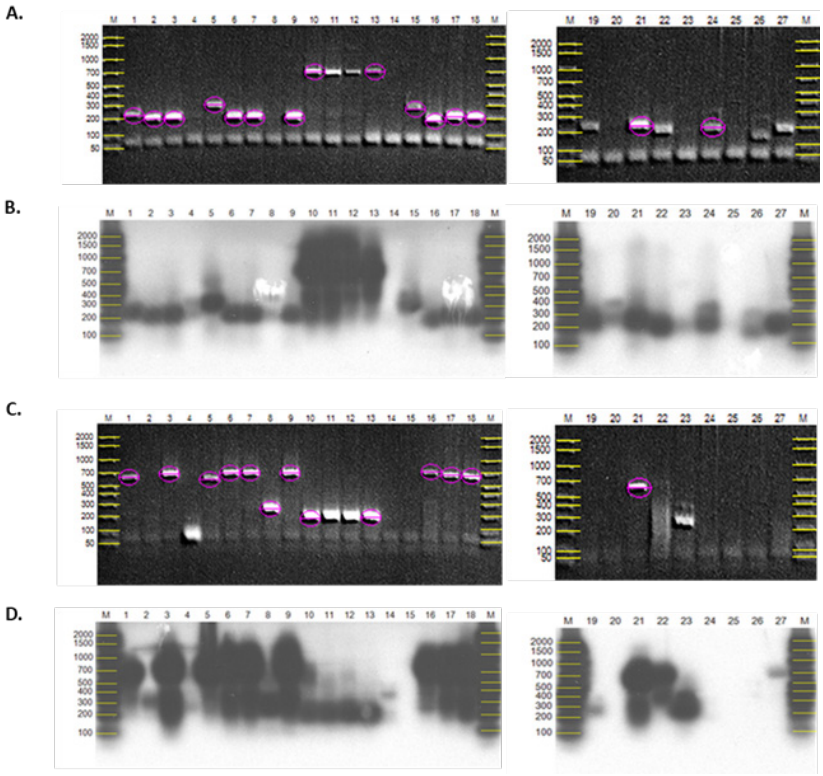

Supplemental Figure S1 - Identification of Mu-insertional alleles using TUSC resources of the Corteva Agriscience. A and C - Gel electrophoresis of the PCR products of F2 plants using a forward GSP (PHN177359) in combination with the Mu-TIR primer and a reverse GSP (PHN177358) in combination with Mu-TIR primer, respectively. B and D - Southern Blot (SB) analysis of the PCR products from A and C electrophoresis gels using a DNA probe from Zm00001d001959 gene amplified by two GSPs, PHN177359 and PHN177358. E and F - Selected PCR bands from gels A and C were excised for cloning and sequencing to determine the Mutator-insertion sites in the Zm00001d001959 genomic sequence.

```
                    10        20        30        40        50        60        70
bm6-ref             ACCCCATCGCTTCGTCGCTA---CGCAGTTCGGTCCACCTATCCTTCCCTCCCTCATCGCGTTTTATTAT
ZmBm6-WT            ACCCCATCGCTTCGTCGCTAGTACGCA
bm6-P48F9           ACCCCATCGCTTCGTCGCTAGTACGCAGTTCGGTCCACCTATC----------------------------------------------------------------------

                    80        90        100       110       120       130       140
bm6-ref             TCCCGTCCTTCTTCATT
ZmBm6-WT
bm6-P48F9           ----------TATCGCCTCCTTGTCGGCCGTCGTTATATTTCGCGGCCGATCCTTGTTCAGTT

                    150       160       170       180       190       200       210
bm6-ref             ----------------------------------------------------CGGCCCTTCGCCGCTGCTATATTTCGCGGCCGCCTTGCCTCCTAATAATAG
ZmBm6-WT
bm6-P48F9                     GTTCCTTTTTCCCCATTTGCGCCCCTTCGTCGCTGCTATATTCCGCGACCGCCT ---CGCCTAATAATAG

                    220       230       240       250       260       270       280
bm6-ref             CCGCCGCGGGCAGTGGATACCGCCACCGCCACCGCCATGGGAGCGCTCGAGGAGGCCCACCTCGCGGCCG
ZmBm6-WT            ----------TGGATACCGACACCGCCACCGCCATGGGAGCGCTCGAGGAGGCCCACCTCGCGGCCG
bm6-P48F9           TCGCCGCGGGCAGTGGAYACCGCGACCGCCACCGTCATGGGAGCGCTCGAGGGGGCCCACCTCGCGGCCG

                    290       300       310       320       330       340       350
bm6-ref             CCGCGTGCGCGTG---CGAGGAGGAGGAGGAAAGCGACTACATCGGCCTCCTCGCAGGGGA---AGCGGC
ZmBm6-WT            CCGCGTGCGCGTG---CGAGGAGGAGGAGGAAAGCGACTACATCGGCTTCCTCGCAGGGGA---AGCGGC
bm6-P48F9           TCGCTTGCGCGTGTGACGATGACGAGGAGCAAAGCGACTGCATCCCCCTGCTCGCAGGGGACGCCGCGAC

                    360       370       380       390       400       410       420
bm6-ref             GGCGGGCGACGCCGTGGAGCCGGCCGTGCGCGCCCTGCTGCTGGGGCTCGGTGAGGACGACCGCCGCGAG
ZmBm6-WT            GGCGGGCGACGCCGTGGAGCCGGCCGTGCGCGCCCTGCTGCTGGGGCTCGGTGAGGACGACCGCCGCGAG
bm6-P48F9           GGCGGCCGACGCCATGGAGCCGGCGGTGCGCGCGCTCCTGCTGGGGCTCGGCGAGGACGACCGCCGCGAG

                    430       440       450       460       470       480       490
bm6-ref             GGCCTGCTCCGGACGCCCAAGCGCGTCGCCAAGGCCTTCCGCGACGGCACCCGAGGCTACAGGCAAAAAG
ZmBm6-WT            GGCCTGCTCCGGACGCCCAAGCGCGTCGCCAAGGCCTTCCGCGACGGCACCCGAGGCTACAGGCAAAAAG
bm6-P48F9           GGACTGCGCCGGACGCCCAAGCGCGTCTCCAAGGCCTTCCGCGACGGCACCCGAGGTTACAGGCAAAAAG

                    570       580       590       600       610       620       630
bm6-ref             AACTGGCGGGCAAGTAGTTGTTCGAGACATTGAACTTTTCTCCTATTGTGAGTCATGCTTGCTTCCATTC
ZmBm6-WT            AACTGGCGGGCAAGTAGTTGTTCGAGACATTGAACTTTTCTCCTATTGTGAGTCATGCTTGCTTCCATTC
bm6-P48F9           AACTGGCGGGCAAGTAGTTGTCCGAGACATTGAACTTTTCTCATACTGCGAGTCATGCTTGCTTCCATTC

                    640       650       660       670       680       690       700
bm6-ref             AGCATACAGTGCCATGTGGGGTATGTTCCCTCAGGTGGAAGAGTGGTTGGGTTAAGCAAGCTTTCTAGAG
ZmBm6-WT            AGCATACAGTGCCATGTCGGGTATGTTCCCTCAGGTGGAAGAGTGGTTGGGTTAAGCAAGCTTTCTAGAG
bm6-P48F9           AGCATACAGTGCCATGTTGGGTATGTTCCCTCGGGTGGAAGGGTGGTTGGGTTAAGCAAGCTTTCTAGAG

                    710       720       730       740       750       760       770
bm6-ref             TATCTGATGTCTTTGCCAAGAGATTGCAAAACCCTCAAAGACTAGCTAATGAAATCTGTGGTGCACTGCA
ZmBm6-WT            TATCTGATGTCTTTGCCAAGAGATTGCAAAACCCTCAAAGACTAGCTAATGAAATCTGTGGTGCACTGCA
bm6-P48F9           TGTCTGATGTCTTTGCCAAGAGATTGCAAAACCCTCAAAGACTAGCCAATGAAGTCTGTGGTGCACTGCA
```

Supplemental Figure S2 - The multiple alignments of the mature transcript sequences of *bm6-P48F9* compared to the *bm6-ref* allele and its wild-type sib. The intronic DNA sequence present in the mature transcripts of *bm6-ref* and *bm6-P48F9* alleles is highlighted by blue letters, whereas the exonic sequence of the ZmGCH1 gene is represented by bold black letters.